Radiation Physics and Chemistry 180 (2021) 109263

Contents lists available at ScienceDirect

Radiation Physics and Chemistry

journal homepage: www.elsevier.com/locate/radphyschem

Isotopic effects in Debye-Waller factor and in EXAFS studied based on anharmonic correlated Einstein model

Nguyen Van Hung [a,*], Nguyen Ba Duc [b], Dinh Quoc Vuong [c], Tong Sy Tien [d], Nguyen Cong Toan [e]

[a] Institute of Research and Development, Duy Tan University, Da Nang, 550000, Viet Nam
[b] Department of Physics, Tan Trao University, Km6, Trung Mon, Yen Son, Tuyen Quang, Viet Nam
[c] Quang Ninh Education & Training Department, Cam Pha School, Ha Long, Quang Ninh, Viet Nam
[d] Department of Basic Sciences, University of Fire, 243 Khuat Duy Tien, Thanh Xuan, Hanoi, Viet Nam
[e] Department of Physics, University of Science, Vietnam National University, Hanoi, 334 Nguyen Trai, Thanh Xuan, Hanoi, Viet Nam

ARTICLE INFO

Keywords:
Isotopic effects
Debye-waller factor
EXAFS
Cumulant expansion approach
Anharmonic correlated einstein model
Ni isotopes

ABSTRACT

Isotopic effects in Debye-Waller factor and in extended X-ray absorption fine structure (EXAFS) have been studied. The studies are succeeded based on anharmonic correlated Einstein model for isotopes derived for providing analytical expressions of cumulants containing isotopic effects and for application of these cumulants to EXAFS of isotopes. Advantageous development here is creation of a method giving not only the isotopic effects but also the considered quantities only from second cumulant. The model is simplified by using one-dimension with taking many-body effects into account based on including nearest neighbor contributions to vibrations between absorber and backscatterer isotopic atoms. Morse potential is assumed to describe single-pair isotopic atomic interaction. Isotopic effects evidenced in cumulants, EXAFS spectra and their Fourier transform magnitudes of Ni isotopes calculated by present theory are found to be in good similarity to those obtained in experimental results of ^{70}Ge and ^{76}Ge.

1. Introduction

Extended X-ray absorption fine structure (EXAFS) has developed into a powerful technique for providing information on local atomic structure and thermal effects of the substances, where the Debye-Waller factor (DWF) accounts for the effects of atomic thermal vibrations. This DWF damps EXAFS spectra with respect to increasing temperature T and wave number k (or energy). The effects concerning temperature and anharmonicity dependence in EXAFS are oft evaluated based on cumulant expansion approach (Crozier et al., 1988). This procedure is successfully applied to several models like the anharmonic correlated Einstein model (ACEM) (Hung and Rehr, 1997), anharmonic correlated Debye model (Hung et al., 2010), path integral calculation (Yokoyama, 1998), force constant model (Poiarkova and Rehr, 1999), dynamic matrix calculation (Vila et al., 2007), EXAFS Mössbauer study (Daniel et al., 2004) and several others. They provide different methods for studying the thermodynamic properties and anharmonic effects of the considered crystals based on DWFs presented in terms of cumulant expansion. In EXAFS experiment, the probes are the individual photoelectrons emitted by X-ray absorbing atoms and backscattered by neighboring atoms. Because of the photoelectrons short range, EXAFS can give original information on the local dynamics of crystals. The dynamical properties of crystals mainly depend on the atomic number of the constituent atoms. The isotopic composition influences on some basic properties, like, density, phonon widths, and electronic energy gaps (Cardona and Thewalt, 2005). The zero-point amplitude of atomic vibrations is also influenced by the nuclear masses. Isotopic effects are relevant not only for their basic scientific interest, but also for several possible technological applications (Plekhanov, 2006).

Many efforts have been made to study the isotopic effects. The dependence of dynamical properties of crystals on isotopic composition is intensively studied (Cardona, 2000). The basic theory of isotopic effect on lattice constants has been derived (London, 1958). The dependence of the lattice constants of some semiconductors has been theoretically evaluated in the quasi-harmonic approximation using phonon frequencies calculated from first principles via density-functional perturbation theory (Pavone and Baroni, 1994). Path-integral Monte Carlo simulations have been performed for isotopes of Ge on the basis of a Stillinger-Weber potential (Noya et al., 1997). EXAFS has been measured on two powdered samples of ^{70}Ge and ^{76}Ge as

* Corresponding author.
E-mail address: hungnv@vnu.edu.vn (N. Van Hung).

https://doi.org/10.1016/j.radphyschem.2020.109263
Received 1 May 2020; Received in revised form 16 September 2020; Accepted 19 October 2020
Available online 10 November 2020

a function of temperature from 20 to 300 K (Purants et al., 2008). Unfortunately, a theoretical work on the calculation and analysis of the isotopic effects, as well as the values of DWFs presented in terms of cumulant expansion and of EXAFS of isotopes is still not available.

The purpose of this work is to study not only the isotopic effects but also the values of DWFs presented in terms of cumulant expansion and of EXAFS of isotopes. The successes of these studies presented in Section 2 are based on the ACEM for isotopes quantum statistically derived with the purposes firstly for providing the analytical expressions of three first EXAFS cumulants containing the isotopic effects, and secondly, for application of these cumulants to study EXAFS of isotopes. The advantageous development in the present theory is creation of a method providing not only the isotopic mass difference effects but also the values of the considered quantities only from those of second cumulant. This model is simplified by using one-dimension with taking the many-body effects into account based on the anharmonic effective potential that includes the interactions of absorber and backscatter isotopic atoms with all their nearest neighbors. Morse potential is assumed to describe the single-pair isotopic atomic interaction. The isotopic effect in each considered quantity is specified in the present theory based on the difference of its values for two different isotopes. The advantage of the present ACEM for isotopes is possibility of its application to any isotopic structure. In Section 3 the derived expressions are applied to numerical calculations for the cumulants, EXAFS spectra and their Fourier transform magnitudes of Ni isotopes. The isotopic mass difference effects neatly evidenced in the considered quantities calculated using the present theory are compared to those obtained in the EXAFS experimental results of isotopes ^{76}Ge and ^{70}Ge (Purants et al., 2008) which show their good similarity. The conclusions are presented in Section 4.

2. Anharmonic correlated Einstein model for isotopes

2.1. Anharmonic effective potential

Let us consider the present ACEM for isotopes characterized by an anharmonic interatomic effective potential expanded to the third order

$$V_{eff}(x) = \frac{1}{2}k_{eff}x^2 + k_{3eff}x^3 + \cdots, \quad x = r - r_0\cdot, \tag{1}$$

where k_{eff} is effective local force constant, k_{3eff} is effective cubic parameter giving an asymmetry of the potential due to anharmonicity, and x is deviation of instantaneous bond length between the two isotopic atoms r from its equilibrium value r_0.

Because isotopes are monatomic the anharmonic effective potential given by Eq. (1) is defined in the present ACEM for isotopes based on an assumption in the center-of-mass frame of single-bond pair of absorber and backscatterer isotopic atoms as

$$V_{eff}(x) = V(x) + \sum_{i=a,b}\sum_{j\neq a,b} V\left(\frac{1}{2}x\widehat{\mathbf{R}}^0\cdot\widehat{\mathbf{R}}_{ij}\right), \tag{2}$$

where the first term on the right concerns only absorber and backscatter isotopic atoms, the remaining sums extend over their nearest neighbors describing the lattice contributions to pair interaction and depends on isotope structure type. Here $\widehat{\mathbf{R}}^0$ is direction unit vector linking absorber and backscatter, and $\widehat{\mathbf{R}}_{ij}$ is the unit vector along the bond between ith and jth atoms.

Comparing Eq. (1) to Eq. (2) the parameters k_{eff} and k_{3eff} of the anharmonic effective potential of isotopes are determined. They are different for different isotopic structures.

Hence, the anharmonic effective pair potential given by Eq. (2) describes not only pair interaction of absorber and backscatter isotopic atoms themselves, but also an effect of their nearest neighbors on such interaction due to that the many-body effects are taken into account. By this way the complicated quantum statistical task of many-body system for isotopes in EXAFS theory is simplified into the one of one-dimensional model.

Note that the anharmonic effective potential method (Hung and Rehr, 1997) has been successfully applied to EXAFS valuations of thermodynamic properties and anharmonic effects of fcc (Hung and Rehr, 1997; Hung et al., 2010; Daniel et al., 2004), bcc (Hung et al., 2016), hcp (Hung et al., 2017) crystals and semiconductors (Toan and Hung, 2019) by providing good agreement between the theoretical and experimental results, and now it is applied to the present ACEM for isotopes.

2.2. EXAFS cumulants containing isotopic effects

Derivation of EXAFS cumulants in the present ACEM for isotopes is based on quantum statistical theory (Feynman, 1972) and the anharmonic effective potential presented in the previous section. The physical quantities are now determined based on an averaging procedure using the canonical partition function Z and statistical density matrix ρ, e.g.,

$$\langle y^m\rangle = \frac{1}{Z}Tr(\rho\, y^m), \quad m = 1, 2, 3, \cdots \tag{3}$$

Atomic vibrations are quantized in terms of phonons, and anharmonicity is the result of phonon-phonon interaction, that is why we express y in terms of the annihilation and creation operators, $\widehat{a}$ and $\widehat{a}^+$, respectively

$$y \equiv a_0(\widehat{a} + \widehat{a}^+), \quad a_0^2 = \hbar\omega_E \,/\, 2k_{eff}, \tag{4}$$

As well as use the harmonic oscillator state $|n\rangle$ as the eigenstate with the eigenvalue $E_n = n\hbar\omega_E$ for n being the phonon number, ignoring the zero-point energy for convenience.

The correlated Einstein frequency ω_E contained in Eq. (4) and then the Einstein temperature θ_E in the present ACEM for isotopes have the following forms

$$\omega_E = \sqrt{2k_{eff}/M}, \quad \theta_E = \hbar\omega_E \big/ k_B, \tag{5}$$

where M is isotopic atomic mass and k_B is Boltzmann constant.

The correlated Einstein frequency ω_E and temperature θ_E given by Eq. (5) contain the mass parameter M describing the isotopic effects based on its difference for different isotopes. It leads to the isotopic effect in the canonical partition function Z included in Eq. (3) which for weak anharmonicity in EXAFS approximates its equilibrium value Z_0 as

$$Z \cong Z_0 = \sum_n e^{-n\beta\hbar\omega_E} = \sum_{n=0}^{\infty} z^n = \frac{1}{1-z}, \; z = \exp(-\theta_E / T), \tag{6}$$

Containing the temperature parameter z depending on correlated Einstein temperature θ_E.

Therefore, the physical quantities determined by Eq. (3) in the present ACEM for isotopes evidently contain the isotopic mass difference effects.

Using the above results for the correlated isotopic atomic vibration and the procedure depicted by Eqs. (3)–(6), as well as the first-order thermodynamic perturbation theory (Feynman, 1972) the temperature-dependent EXAFS cumulants in the present ACEM for isotopes have been derived.

Consequently, the EXAFS cumulants in the present ACEM for isotopes have resulted for the first cumulant describing net thermal expansion or isotopic lattice disorder

$$\sigma^{(1)}(T) = a = \sigma_0^{(1)}\frac{1+z(T)}{1-z(T)} = \frac{\sigma_0^{(1)}}{\sigma_0^2}\sigma^2(T), \; \sigma_0^{(1)} = -\frac{3k_{3eff}}{k_{eff}}\sigma_0^2, \tag{7}$$

For the second cumulant describing mean square relative displacement (MSRD)

$$\sigma^2(T) = \langle y^2\rangle = \sigma_0^2\frac{1+z(T)}{1-z(T)}, \; \sigma_0^2 = \frac{\hbar\omega_E}{2k_{eff}}, \tag{8}$$

And for the third cumulant or mean cubic relative displacement (MCRD) describing the asymmetry of the pair distribution function

$$\sigma^{(3)}(T) = \langle y^3 \rangle = \sigma_0^{(3)} \left[3\left(\sigma^2(T)/\sigma_0^2\right)^2 - 2 \right], \ \sigma_0^{(3)} = -\frac{2k_{3eff}}{k_{eff}}\left(\sigma_0^2\right)^2. \quad (9)$$

From the above results we obtain a simple relation between cumulants for the present model

$$\frac{\sigma^{(1)}\sigma^2}{\sigma^{(3)}} = \frac{1}{2 - (4/3)(\sigma_0^2/\sigma^2)^2}. \quad (10)$$

In the above obtained expressions $\sigma_0^{(1)}$, σ_0^2, $\sigma_0^{(3)}$ are zero-point energy contributions to the cumulants $\sigma^{(1)}$ (T), σ^2(T), $\sigma^{(3)}$ (T), respectively.

Note that the obtained cumulants given by Eq. (7) – (9) and their relation given by Eq. (10) in the present ACEM for isotopes contain the isotopic mass difference effects simply based on the presentation of these quantities in terms of second cumulant given by Eq. (8) including the correlated Einstein frequency ω_E given by Eq. (5) and the temperature parameter z given by Eq. (6) containing the isotopic mass difference effects. Such advantage leads to creating a method providing not only the isotopic effects but also the values of the considered quantities only from the second cumulant. Moreover, this method also leads to significant reduction of numerical calculations of the considered quantities based on only the calculation of second cumulant. It will be used in Section 3 for numerical calculations of the considered quantities.

2.3. Low- and high-temperature limit

It is useful to consider the low-temperature (LT) and high-temperature (HT) limits of the considered quantities in the present ACEM for isotopes. In the LT limit z → 0, so that the terms with z^2 and higher powers can be neglected, and in the HT limit it is approximated that $z \cong 1 - \hbar\omega_E/k_BT$. Using these approximations the expressions of cumulants given by Eqs. (7)–(9) and their relation given by Eq. (10) have been transformed into those for the LT and HT limits which are written in Table 1.

2.4. Application to EXAFS of isotopes

The cumulants derived in the previous section can be applied to EXAFS of isotopes whose expression according to the cumulant expansion approach is given by

$$\chi(k) = \frac{S_0^2 N}{kR^2} F(k) e^{-2R/\lambda(k)} \mathrm{Im}\left\{ e^{i\Phi(k)} \exp\left[2ikr_0 + \sum_{n=1}^{\infty} \frac{(2ik)^n}{n!}\sigma^{(n)}(T) \right] \right\}, \quad (11)$$

where k and λ are the wave number and mean free path of emitted photoelectron, respectively, F(k) is the real atomic backscattering amplitude, $\Phi(k)$ is net phase shift, N is atomic number of a shell, S_0^2 is the intrinsic loss factor due to many-electron effects, $R = \langle r \rangle$ with r being the instantaneous bond length between absorber and backscatterer isotopic atoms, r_0 is the equilibrium value of r, and $\sigma^{(n)}$ (n = 1, 2, 3, …) are the cumulants describing DWFs.

Note that the cumulants contained in the EXAFS expression given by Eq. (11) can be presented in terms of second cumulant containing the isotopic mass difference effects as it was done in section 2.2. This leads to including the isotopic effects in EXAFS spectra and their Fourier transform magnitudes based only on those of second cumulant. By such way we also can simplify the calculation and analysis of the considered quantities using the present ACEM for isotopes.

Table 1
Three first EXAFS cumulants $\sigma^{(1)}$, σ^2, $\sigma^{(3)}$ and their relation $\sigma^{(1)}\sigma^2/\sigma^{(3)}$ of isotopes in the LT (T → 0) and HT (T → ∞) limits.

Quantities	T → 0	T → ∞
$\sigma^{(1)}$	$\sigma_0^{(1)}(1 + 2z)$	$-3k_{3eff}k_BT/k_{eff}^2$
σ^2	$\sigma_0^2(1 + 2z)$	k_BT/k_{eff}
$\sigma^{(3)}$	$\sigma_0^{(3)}(1 + 12z)$	$-6k_{3eff}(k_BT)^2/k_{eff}^3$
$\sigma^{(1)}\sigma^2/\sigma^{(3)}$	$3(1 + 2z)^2/2(1 + 12z)$	1/2

Note from Table 1 that at high-temperatures the cumulants $\sigma^{(1)}$, σ^2, $\sigma^{(3)}$ and their relation $\sigma^{(1)}\sigma^2/\sigma^{(3)}$ of isotopes approach their classical values which do not contain the isotopic mass difference parameters describing the isotopic effects. But at low-temperatures the cumulants $\sigma^{(1)}$, σ^2, $\sigma^{(3)}$ and their relation $\sigma^{(1)}\sigma^2/\sigma^{(3)}$ contain zero-point energy contributions $\sigma_0^{(1)}$, $\sigma_0^{(2)}$, $\sigma_0^{(3)}$ and the parameter z so that they evidently contain the isotopic mass difference effects.

3. Numerical results and discussions

Now we apply the expressions derived in the previous section to numerical calculations for Ni and its isotopes.

Based on fcc structure of Ni and its isotopes the anharmonic effective potential given by Eq. (2) has been calculated and resulted as

$$V_{eff}^{fcc}(x) = V(x) + 2V\left(-\frac{x}{2}\right) + 8V\left(-\frac{x}{4}\right) + 8V\left(\frac{x}{4}\right). \quad (12)$$

Applying the Morse potential expanded up to the third order around its minimum

$$V(x) = D\left(e^{-2\alpha x} - 2e^{-\alpha x}\right) = D\left(-1 + \alpha^2x^2 - \alpha^3x^3 + \cdots\right), \quad (13)$$

where α describes the width of the potential and D is the dissociation energy, to Eq. (12), as well as comparing the result to Eq. (1) the parameters k_{eff} and k_{3eff} of effective potential given by Eq. (12) for Ni and its isotopes presented in terms of Morse potential parameters are determined.

For Ni we have D = 0.4205 eV, α = 1.4199 $Å^{-1}$ (Girifalco and Weizer, 1959) which were obtained using experimental values for the energy of sublimation, the compressibility, the lattice constant and are applied to all Ni isotopes because of Morse potential independence on atomic mass. They have been used to calculate the effective local force constant k_{eff}, effective anharmonic cubic parameter k_{3eff}, correlated Einstein frequency ω_E and temperature θ_E, and then three first EXAFS cumulants of Ni and its isotopes ^{68}Ni, ^{50}Ni, ^{40}Ni. Some results are written in Table 2.

Table 2 shows the different values of correlated Einstein frequency ω_E and temperature θ_E, second cumulant $\sigma^2(T = 65\,K)$ and interatomic distance $R(T = 65\,K)$ of isotopes ^{68}Ni, ^{50}Ni, ^{40}Ni calculated using the present theory. They increase as the atomic mass numbers of isotopes decrease. These results illustrate the clear dependence of the considered quantities on atomic mass numbers of isotopes describing the evidenced isotopic mass difference effects of these considered quantities calculated using the present theory. The equality of the effective local force constants k_{eff} of all considered Ni isotopes is similar to the one of local force constants obtained in EXAFS experiment of isotopes ^{76}Ge and ^{70}Ge (Purants et al., 2008). We apply here the average interatomic distance in the form $R(T) = \langle r \rangle = r_0 + \sigma^{(1)}(T)$ (Yokoyama et al., 1996) so that its accuracy is limited due to not including the perpendicular MSRD (Fornasini et al., 2004) which can not be solely obtained from EXAFS. It requires comparison to the three-dimensional XRD technique.

The isotopic mass difference effects described by the dependence of the correlated Einstein frequencies ω_E and temperatures θ_E of Ni and its isotopes ^{68}Ni, ^{64}Ni, ^{50}Ni, ^{40}Ni on their atomic mass M calculated using

Table 2
The values of k_{eff}, ω_E, θ_E, $\sigma^2(T = 65\,K)$, interatomic distance $R(T = 65\,K)$ of isotopes^{68}Ni,^{50}Ni,^{40}Ni calculated using the present theory.

Isotopes	$k_{eff}(N/m)$	$\omega_E(10^{+13}\mathrm{Hz})$	θ_E(K)	$\sigma^2(Å^2)$	R(Å)
^{64}Ni	6.915	3.5646	272.2843	0.0029	2.4920
^{50}Ni	6.915	4.0329	308.0545	0.0032	2.4924
^{40}Ni	6.915	4.5089	344.4154	0.0035	2.4928

the present theory are also clearly seen in Fig. 1a for ω_E and in Fig. 1b for θ_E. Here ω_E and θ_E decrease as the atomic mass M of isotopes increases. These isotopic effects are similar to those obtained in the EXAFS experimental results of isotopes ^{76}Ge and ^{70}Ge (Purants et al., 2008).

The correlated Einstein frequency ω_E and temperature θ_E calculated and presented in Fig. 1a and b and have been used for calculating the second cumulant. Fig. 2a illustrates temperature-dependent second cumulants $\sigma^2(T)$ or MSRDs of Ni and its isotopes ^{64}Ni, ^{58}Ni, ^{40}Ni calculated using the present theory. Their clear differences describing the evidenced isotopic mass difference effects are valuated in the present theory based on the temperature-dependent differences $\Delta\sigma^2(T)$ for two different isotopes, e.g., $\sigma^2(^{64}Ni) - \sigma^2(^{40}Ni)$ and $\sigma^2(^{64}Ni) - \sigma^{(1)}(^{50}Ni)$ (Fig. 2b). Both curves presented in Fig. 2b for these values describing the isotopic mass difference effects in second cumulant $\sigma^2(T)$ or MSRDs are significant at low-temperatures. They decrease as the temperature increases and approach zero-values indicating the disappearance of the isotopic effects at high-temperatures as it was obtained in the EXAFS experimental results of isotopes ^{76}Ge and ^{70}Ge (Purants et al., 2008).

Further, we use the calculated second cumulants presented in Fig. 2a to obtain the results for the other considered quantities calculated using the present theory. Fig. 3a shows temperature-dependent first cumulant $\sigma^{(1)}(T)$ of Ni and its isotopes ^{64}Ni, ^{50}Ni, ^{40}Ni describing the net thermal expansion or lattice disorder of these isotopes. The significant differences between $\sigma^{(1)}(T)$ for the considered isotopes ^{64}Ni, ^{50}Ni, ^{40}Ni (Fig. 3a) describing their isotopic mass difference effects are valuated in the present theory based on the temperature-dependent differences $\Delta\sigma^{(1)}$ for two different isotopes, e.g., $\sigma^{(1)}(^{64}Ni) - \sigma^{(1)}(^{40}Ni)$ and $\sigma^{(1)}(^{64}Ni) - \sigma^{(1)}(^{50}Ni)$ (Fig. 3b). The isotopic mass difference effects of $\sigma^{(1)}(T)$ presented in Fig. 3a and b are significant at low-temperatures. They decrease as the temperature increases and disappear at high-temperatures (both curves describing $\sigma^{(1)}(^{64}N) - \sigma^{(1)}(^{40}Ni)$ and $\sigma^{(1)}(^{64}Ni) - \sigma^{(1)}(^{50}Ni)$ in Fig. 3b approach zero-values).

Note that the isotopic mass difference effects obtained in temperature-dependent ineratomic distance R(T) of isotopes ^{64}Ni, ^{50}Ni, ^{40}Ni calculated using the present theory are totally similar to those of $\sigma^{(1)}(T)$ because R(T) is obtained from the expression $R\ (T) = \langle r\rangle = r_0 + \sigma^{(1)}(T)$ (Yokoyama et al., 1996). Here, $\Delta R(T) = \Delta\sigma^{(1)}(T)$ so that the isotopic mass difference effects in the ineratomic distance R(T) of isotopes ^{64}Ni, ^{50}Ni, ^{40}Ni are the same as those of $\sigma^{(1)}(T)$ presented in Fig. 3b.

Temperature-dependent third cumulant $\sigma^{(3)}(T)$ of isotopes ^{64}Ni, ^{58}Ni, ^{40}Ni describing MCRD or the asymmetry of pair-distribution function of the considered isotopes are presented in Fig. 4a. They are about the same as the one of Ni. Their differences describing the isotopic effects are negligible. It is understandable because the anharmonicity is dominant at high-temperatures (see Stern et al., 1991; Hung and Rehr, 1997), but the isotopic mass difference effects disappear at these high-temperatures. Such property of $\sigma^{(3)}(T)$ for Ni isotopes is similar to the one obtained in the EXAFS experimental results of isotopes ^{76}Ge and ^{70}Ge (Purants et al., 2008).

The cumulant relation $\sigma^{(1)}\sigma^2/\sigma^{(3)}$ is oft considered in EXAFS studies (see for example Stern et al., 1991; Hung and Rehr, 1997). It is equal to 1.5 at T = 0 K and approach the constant value of 1/2 at high-temperatures for fcc crystals (Hung and Rehr, 1997). The calculated results using the present theory for this relation of isotopes ^{64}Ni, ^{58}Ni, ^{40}Ni presented in Fig. 4b are very different showing significant isotopic mass difference effects at low-temperatures. These isotopic effects decrease as the temperature increases and disappear at high-temperatures (all curves approach the classical value of 1/2) (Stern et al., 1991).

Note that the obtained values presented in the above figures for the cumulants and their relation of Ni isotopes show their clear dependence on isotopic atomic mass numbers. They increase as the isotopic atomic mass numbers decrease as in the EXAFS experimental results of isotopes ^{76}Ge and ^{70}Ge (Purants et al., 2008) where σ^2 of ^{70}Ge is greater σ^2 of ^{76}Ge.

Further, we consider the isotopic mass difference effects in EXAFS calculated using the present theory. Based on the above obtained cumulants presented in terms of second cumulant containing the isotopic mass difference effects we calculated EXAFS spectra of isotopes ^{64}Ni, ^{58}Ni, ^{40}Ni at T = 25 K (Fig. 5a) and their Fourier transform magnitudes (Fig. 5b) using the FEFF code (Rehr et al., 1991) modified by adding our expressions for the cumulants containing the isotopic effects. These obtained EXAFS spectra and their Fourier transform magnitudes are clearly different showing their isotopic mass difference effects. These isotopic mass difference effects appear only at a low-temperature (T = 25 K). Moreover, they are obtained only in the EXAFS amplitudes and in the peak heights of their Fourier transform magnitudes, but there is only a negligible phase shift of these quantities. It is understandable because the isotopic mass difference effects of second cumulant contributing to EXAFS amplitude are significant, but those of third cumulant contributing to EXAFS phase are negligible. The isotopic mass difference effects evidenced in Fourier transform magnitudes of EXAFS spectra of isotopes ^{64}Ni, ^{58}Ni, ^{40}Ni calculated using the present theory here are also similar to those obtained in the EXAFS experimental results of isotopes ^{76}Ge and ^{70}Ge (Purants et al., 2008).

Note that the isotopic mass difference effects evidenced in the obtained EXAFS spectra and their Fourier transform magnitudes of isotopes ^{64}Ni, ^{58}Ni, and ^{40}Ni come from the cumulants contained in EXAFS equation given by Eq. (11) so that they also are significant at low-temperatures, decrease as the temperature increases and disappear at

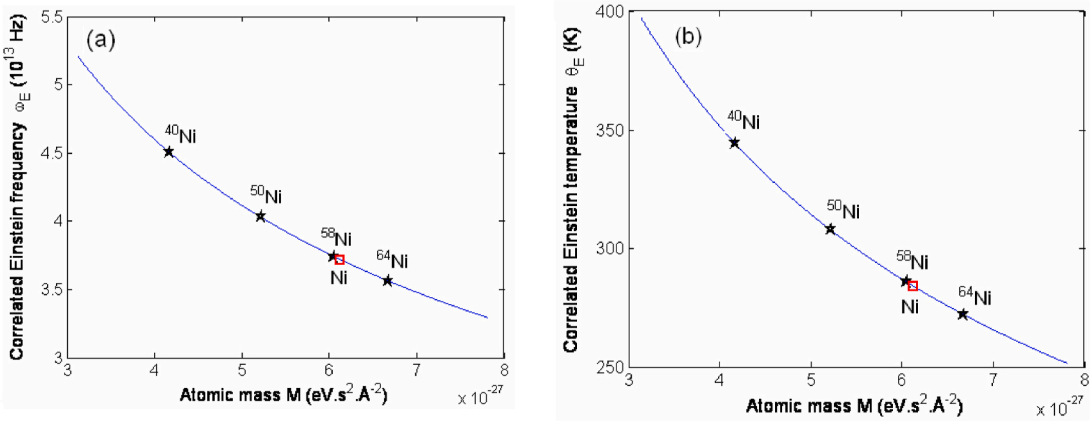

Fig. 1. Dependence of correlated Einstein (a) frequencies ω_E and (b) temperatures θ_E of Ni and its isotopes ^{68}Ni, ^{64}Ni, ^{50}Ni, ^{40}Ni on their atomic mass M calculated using the present theory.

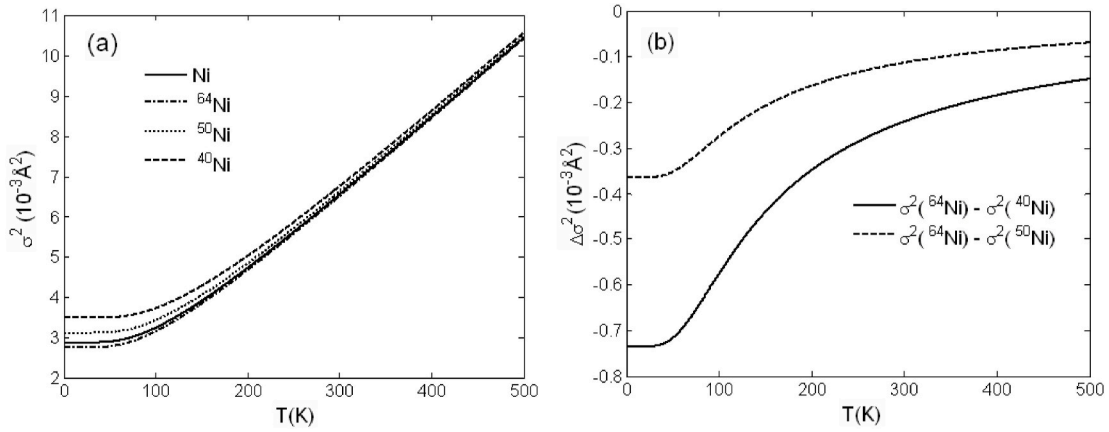

Fig. 2. Temperature-dependent (a) second cumulant $\sigma^2(T)$ of Ni and its isotopes ^{64}Ni, ^{58}Ni, ^{40}Ni and (b) differences $\Delta\sigma^2(T)$ for two different isotopes, e.g., $\sigma^2(^{64}Ni) - \sigma^2(^{40}Ni)$ and $\sigma^2(^{64}Ni) - \sigma^{(1)}(^{50}Ni)$ calculated using the present theory.

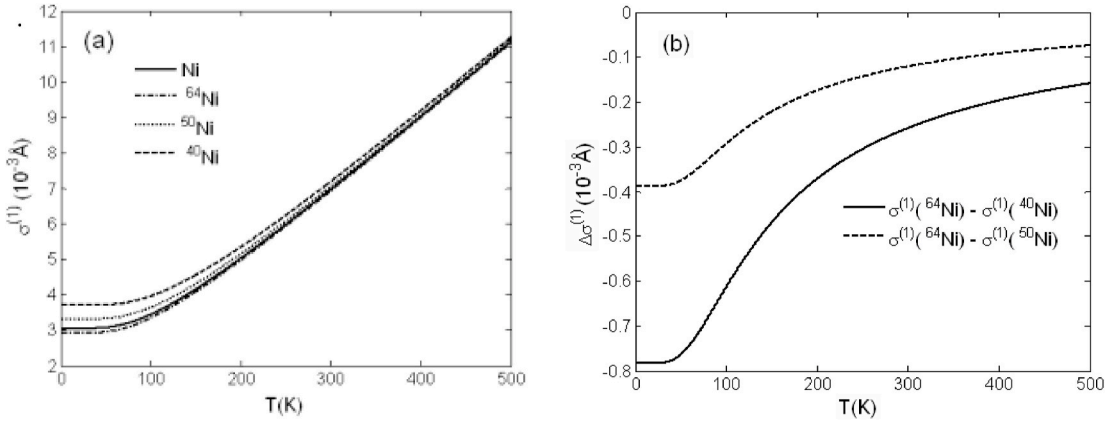

Fig. 3. Temperature-dependent (a) first cumulant $\sigma^{(1)}(T)$ of Ni and its isotopes ^{64}Ni, ^{50}Ni, ^{40}Ni, and (b) differences $\Delta\sigma^{(1)}(T)$ for two different isotopes, e.g., $\sigma^{(1)}(^{64}Ni) - \sigma^{(1)}(^{40}Ni)$ and $\sigma^{(1)}(^{64}Ni) - \sigma^{(1)}(^{50}Ni)$ calculated using the present theory.

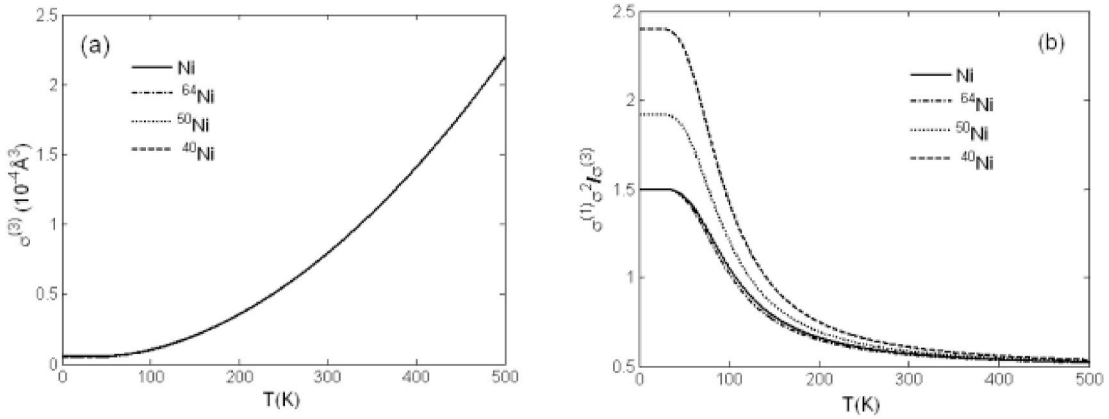

Fig. 4. Temperature-dependent (a) third cumulant $\sigma^{(3)}(T)$ and (b) cumulant relation $\sigma^{(1)}\sigma^2/\sigma^{(3)}$ of Ni and its isotopes ^{64}Ni, ^{58}Ni, ^{40}Ni calculated using the present theory.

high-temperatures as the properties of these cumulants discovered above. Moreover, the peak of Fourier transform magnitude of ^{64}Ni is higher the one of ^{58}Ni as in the EXAFS experimental results of isotopes ^{76}Ge and ^{70}Ge (Purants et al., 2008) where the peak of Fourier transform magnitude of ^{76}Ge is higher the one of ^{70}Ge. It is also understandable because the DWF (second cumulant) damps EXAFS spectrum. Here the second cumulant of ^{58}Ni is greater the one of ^{64}Ni so that its EXAFS spectrum is more damped leading to its peak of Fourier transform magnitude lower the one of ^{64}Ni.

4. Conclusions

In this work the ACEM for isotopes has been quantum statistically derived for the calculation and analysis of not only the isotopic mass

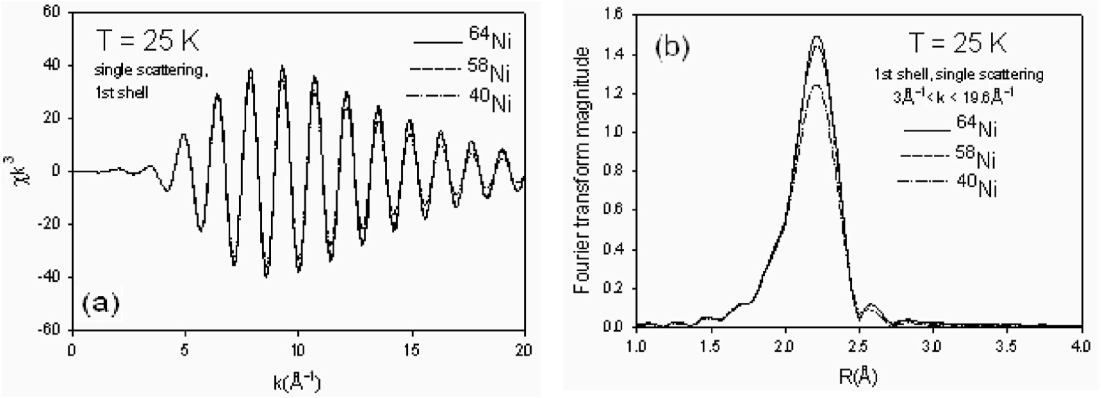

Fig. 5. (a) EXAFS spectra and (b) their Fourier transform magnitudes of isotopes ^{64}Ni, ^{58}Ni, ^{40}Ni at T = 25 K calculated using the present theory.

difference effects but also the values of DWFs presented in terms of cumulant expansion, EXAFS spectra and their Fourier transform magnitudes containing the isotopic effects. The model has the advantage shown by possibility of its application to any isotopic structure.

The derived ACEM for isotopes has successfully simplified the quantum statistical task of many-body system for isotopes in EXAFS theory into the one of one-dimensional model with taking the many-body effects into account based on including the nearest neighbor contributions to the vibrations between absorber and backscatterer isotopic atoms. Here Morse potential is assumed to describe the single-pair isotopic atomic interaction.

The advantageous development in the present theory is creation of a method providing not only the isotopic mass difference effects but also the values of the considered quantities only from those of second cumulant. This method leads to significant reduction of numerical calculations and to simplification of analysis of the considered quantities.

The derived theory is successfully applied to the calculation and analysis of the isotopic effects and the values of DWFs presented in terms of cumulant expansion, EXAFS spectra and their Fourier transform magnitudes of Ni isotopes. Moreover, the dependence of the calculated quantities on isotopic atomic mass numbers where the correlated Einstein frequency and temperature, three first cumulants, interatomic distance increase as the atomic mass numbers decrease leads to a conclusion that the lighter isotopes undergo lager oscillations than the heavier ones. All these results influence on the thermodynamic properties and structural determination of the considered isotopes.

The isotopic mass difference effects in DWFs presented in terms of cumulant expansion and in EXAFS are significant only at low-temperatures where the zero-point amplitude of atomic vibrations plays an important role. They decrease as temperature increases and disappear at high-temperatures. Hence, the isotopic mass difference effects can be evaluated only by quantum theory.

The isotopic mass difference effects evidenced in correlated Einstein frequency and temperature, in DWFs presented in terms of cumulant expansion, in interatomic distance, EXAFS spectra and their Fourier transform magnitudes of Ni isotopes calculated using the present theory are found to be in good similarity to those obtained in the EXAFS experimental results of isotopes ^{76}Ge and ^{70}Ge. This illustrates the efficiencies and simplicity of the present theory in EXAFS studies of isotopic mass difference effects in the considered physical quantities.

Declaration of competing interest

The authors declare that they have no known competing financial interests or personal relationships that could have appeared to influence the work reported in this paper.

Acknowledgments

The authors thank Prof. J. J. Rehr and Prof. P. Fornasini for useful comments.

Appendix A. Supplementary data

Supplementary data to this article can be found online at https://doi.org/10.1016/j.radphyschem.2020.109263.

References

Cardona, M., 2000. Ann. Phys. 9, 865.
Cardona, W., Thewalt, M.L.W., 2005. Rev. Mod. Phys. 77, 1173.
Crozier, E.D., Rehr, J.J., Ingalls, R., 1988. In: Koningsberger, D.C., Prins, R. (Eds.), X-ray Absorption. Wiley, New York.
Daniel, M., Pease, D.M., Hung, N.V., Budnick, J.I., 2004. Local force constants of transition metal dopants in a nickel host: comparison to Mossbauer studies. Phys. Rev. B 69, 134414.
Feynman, R.F., 1972. In: Jacob Shaham, W.A. (Ed.), Statistical Mechanics. Benjamin, INC. Advanced book Program, Reading, Massachusetts.
Fornasini, P., a Beccara, S., Dalba, S., Grisenti, G.R., Samson, A., Vaccari, M., Rocca, F., 2004. EXAFS measurements of copper: local dynamics, anharmonicity, and thermal expansion. Phys. Rev. B 70, 74301.
Girifalco, L.A., Weizer, W.G., 1959. Application of the Morse potential function to cubic metals. Phys. Rev. 114, 687.
Hung, N.V., Rehr, J.J., 1997. Anharmonic correlated Einstein model Debye-Waller factors. Phys. Rev. B 56, 43.
Hung, N.V., Trung, N.B., Kirchner, B., 2010. Anharmonic correlated Debye model Debye-Waller factors. Physica B 405, 2519.
Hung, N.V., Hue, T.T., Khoa, H.D., Vuong, D.Q., 2016. Anharmonic correlated Debye model high-order expanded interatomic effective potential and Debye-Waller factors of bcc crystals. Phys. B 503, 174.
Hung, N.V., Thang, C.S., Duc, N.B., Vuong, D.Q., Tien, T.S., 2017. Temperature dependence of theoretical and experimental Debye-Waller factors, thermal expansion and XAFS of metallic Zinc. Phys. B 521, 198.
London, H., 1958. Z. Phys. Chem. Neue Folge 16, 302.
Noya, J.C., Herrero, C.P., Ramirez, R., 1997. Phys. Rev. B 56, 237.
Pavone, P., Baroni, S., 1994. Solid State Commun. 90, 295.
Plekhanov, V.G., 2006. Prog. Matter Sci. 51, 287.
Poiarkova, A.V., Rehr, J.J., 1999. Multiple scattering x-ray absorption fine structure Debye-Waller factor calculations. Phys. Rev. B 59, 948.
Purants, J., Afify, N.D., Dalba, G., Grisenti, R., De Panfilis, S., Kuzmin, A., Ozohomin, V. I., Rocca, F., Samson, A., Tiutiunnikov, S.I., Fornasini, P., 2008. Isotopic effects in extended x-ray fine structure of germanium. Phys. Rev. Lett. 100, 055901.
Rehr, J.J., Mustre de Leon, J., Sabinsky, S.I., Albert, R.C., 1991. Theoretical x-ray absorption fine structure standards. J. Am. Chem. Soc. 113, 5135.
Stern, E.A., Livins, P., Zhang, Zhe, 1991. Thermal vibration and melting from local perspective. Phys. Rev. B 43, 8850.
Toan, N.C., Hung, N.V., 2019. Temperature-dependence of debye-waller factors of semiconductors presented in terms of cumulant expansion. Glob. J. Engineer. Sci. 3 (5), 1–6.
Vila, F.D., Rehr, J.J., Rossner, H.H., Krappe, H.J., 2007. Theoretical x-absorption fine structure Debye-Waller factors. Phys. Rev. B 76, 014301.
Yokoyama, T., 1998. Path-integral effective-potential method applied to EXAFS cumulants. Phys. Rev. B 57, 3423.
Yokoyama, T., Kobayashi, K., Ohta, T., Ugawa, A., 1996. Anharmonic interatomic potentials of diatomic and linear triatomic molecules studied by EXAFS. Phys. Rev. B 53, 6111.